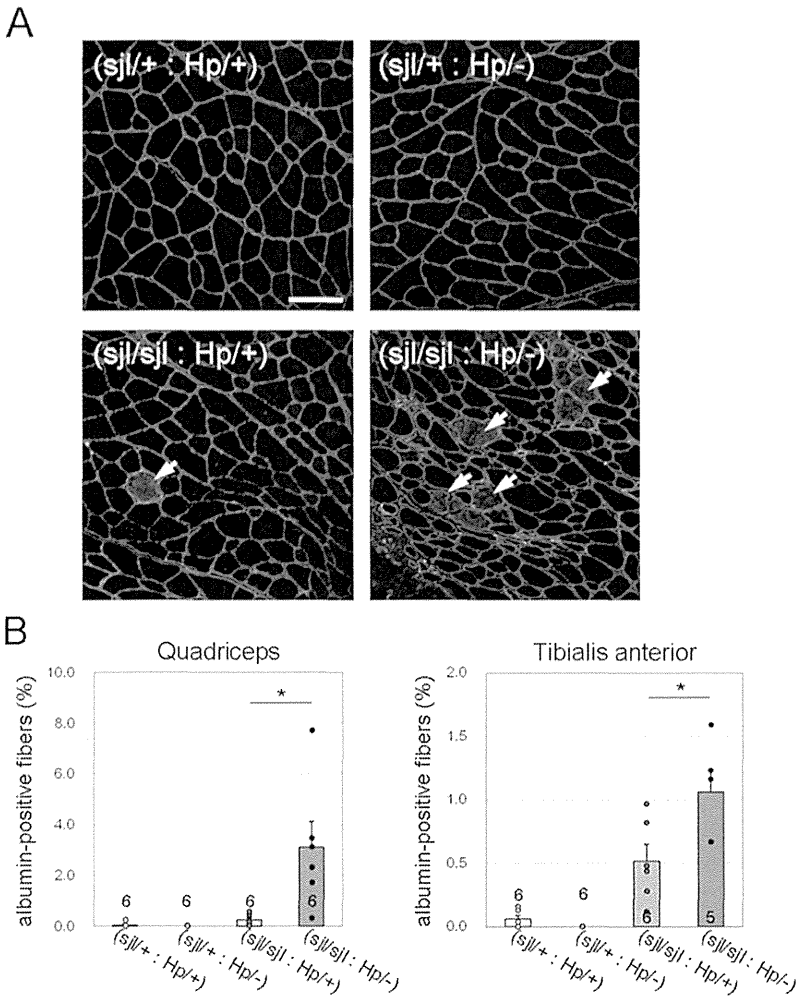

Figure 5. Myofiber membrane fragility in dysferlin/fukutin double mutant mice. (A) Intracellular albumin was determined by immunofluorescence (red). Myofibers are marked by laminin staining (green). Arrows indicate myofibers with intracellular albumin. Images were taken from quadriceps muscle sections of 15-week-old mice. Bar, 100 μm. (B) Myofibers with intracellular albumin were counted and statistically compared between (*dysferlin*$^{sjl/sjl}$: *fukutin*$^{Hp/+}$) and (*dysferlin*$^{sjl/sjl}$: *fukutin*$^{Hp/-}$) mice. Quadriceps and TA muscle sections from 15-week-old mice were analyzed. Data shown are mean ± s.e.m. for each group (*n* is indicated in the graph; *, $p<0.05$). The (*dysferlin*$^{sjl/+}$: *fukutin*$^{Hp/+}$), (*dysferlin*$^{sjl/+}$: *fukutin*$^{Hp/-}$), (*dysferlin*$^{sjl/sjl}$: *fukutin*$^{Hp/+}$), and (*dysferlin*$^{sjl/sjl}$: *fukutin*$^{Hp/-}$) mice are abbreviated as (sjl/+: Hp/+), (sjl/+: Hp/−), (sjl/sjl: Hp/+), and (sjl/sjl: Hp/−), respectively.

doi:10.1371/journal.pone.0106721.g005

Discussion

Here we have characterized the contribution of dysferlin-deficiency to the pathology of dystroglycanopathy using double mutant mice for dysferlin and α-DG glycosylation. To date, several dystroglycanopathy model mice have been established. *Large*^{myd} mice [28] and knock-in mice carrying the FKRP P448L mutation [32] show no detectable amounts of functionally glycosylated α-DG, no laminin binding activity, and progressive muscular dystrophy. On the other hand, other dystroglycanopathy mouse models do not show a muscular dystrophy phenotype [23]. We previously reported that a small amount of intact α-DG in *fukutin*$^{Hp/-}$ mice is sufficient to maintain muscle cell integrity, thus preventing muscular dystrophy [23]. These results and others suggest that the presence of functionally glycosylated α-DG can decrease disease severity [33,34]. In the present study, however, we showed that although (*dysferlin*$^{sjl/+}$: *fukutin*$^{Hp/-}$) mice did not exhibit a muscular dystrophy phenotype, (*dysferlin*$^{sjl/sjl}$: *fukutin*$^{Hp/-}$) mice developed a more exacerbated phenotype than did the *dysferlin* single-mutant (*dysferlin*$^{sjl/sjl}$: *fukutin*$^{Hp/+}$) mice. It has been widely accepted that α-DG glycosylation plays an important role in preventing disease-causing membrane fragility by maintaining a tight association between the basement membrane and the muscle cell membrane, and its defects produce muscle membrane that is susceptible to damage [24,29]. The synergically exacerbated phenotype of the (*dysferlin*$^{sjl/sjl}$: *fukutin*$^{Hp/-}$) mice suggests latent membrane fragility in *fukutin*-deficient *fukutin*$^{Hp/-}$ skeletal muscle. Indeed, the increased number of intracellular albumin-positive fibers in the (*dysferlin*$^{sjl/sjl}$: *fukutin*$^{Hp/-}$) mice also supports this hypothesis. It is assumed in the *fukutin*$^{Hp/-}$ myofiber that interaction between the basement membrane and the cell membrane may be weakened, and therefore disease-causative membrane damage could occur during

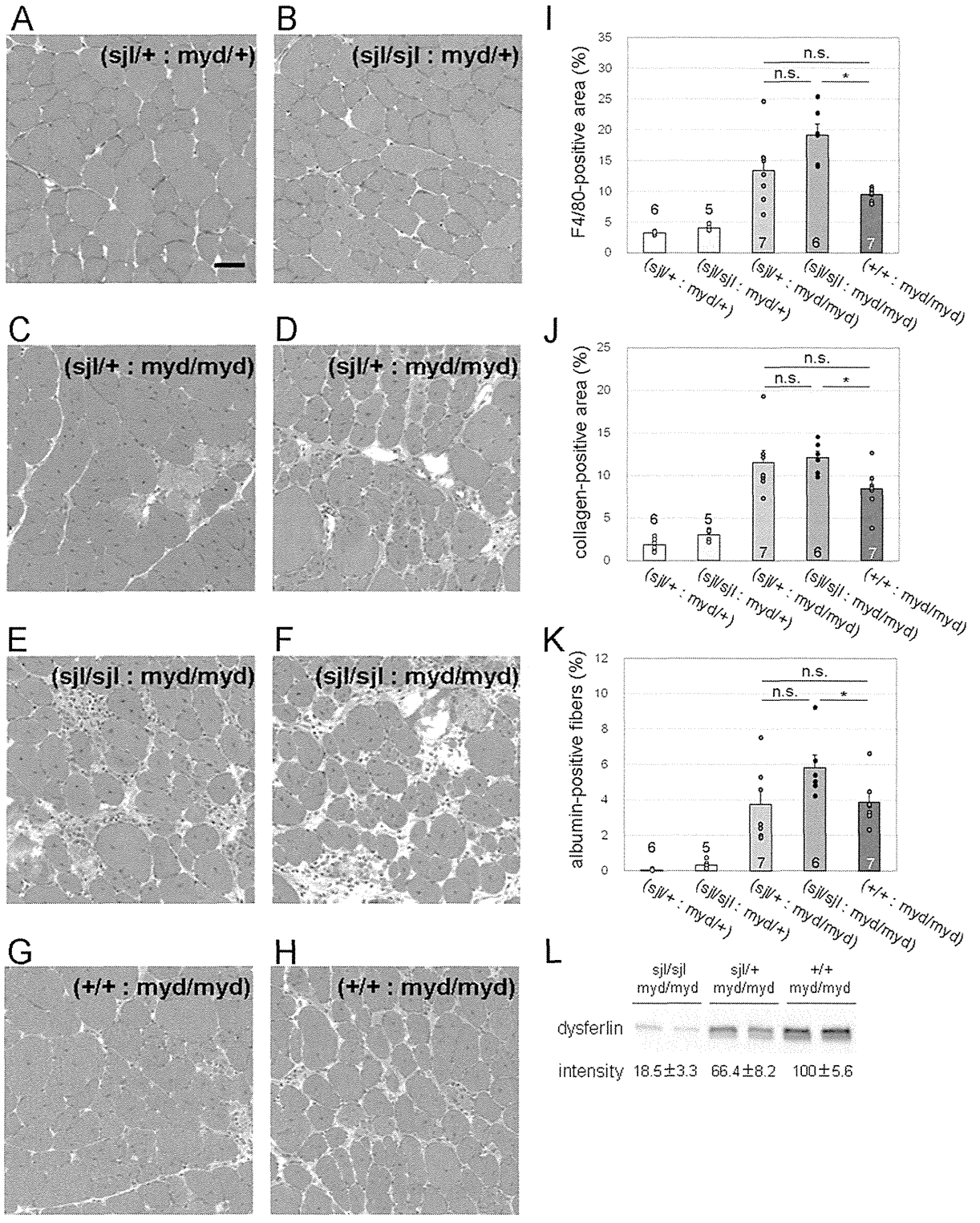

Figure 6. Histopathological analysis of skeletal muscle from dysferlin/Large double mutant mice. (A–H) H&E staining of TA muscle from [(*dysferlin*$^{sjl/+}$: *Large*$^{myd/+}$), A], [(*dysferlin*$^{sjl/sjl}$: *Large*$^{myd/+}$), B], [(*dysferlin*$^{sjl/+}$: *Large*$^{myd/myd}$), C and D], [(*dysferlin*$^{sjl/sjl}$: *Large*$^{myd/myd}$), E and F], and [(*dysferlin*$^{+/+}$: *Large*$^{myd/myd}$), G and H] mice at 15 weeks. Bar, 50 μm. (I) Quantitative analysis of macrophage infiltration, determined by immunofluorescence analysis using F4/80 antibody. (J) Quantitative analysis of connective tissue infiltration determined by immunofluorescence analysis using

anti-collagen I antibody. (K) Quantitative analysis of the proportion of myofibers containing intracellular albumin. For quantitative analysis (I–K), data shown are mean ± s.e.m. for each group (*n* is indicated in the graph; *, $p<0.05$; n.s., not significant). (L) Western blot analysis and quantification of dysferlin expression in the total skeletal muscle lysate from (*dysferlin*$^{sjl/sjl}$: *Large*$^{myd/myd}$), (*dysferlin*$^{sjl/+}$: *Large*$^{myd/myd}$), and (*dysferlin*$^{+/+}$: *Large*$^{myd/myd}$) mice. A representative two individual samples are shown in the blot. Data shown are the average of three individual mice with standard deviations. The (*dysferlin*$^{sjl/+}$: *Large*$^{myd/+}$), (*dysferlin*$^{sjl/sjl}$: *Large*$^{myd/+}$), (*dysferlin*$^{sjl/+}$: *Large*$^{myd/myd}$), (*dysferlin*$^{sjl/sjl}$: *Large*$^{myd/myd}$), and (*dysferlin*$^{+/+}$: *Large*$^{myd/myd}$) mice are abbreviated as (sjl/+: myd/+), (sjl/sjl: myd/+), (sjl/+: myd/myd), (sjl/sjl: myd/myd), and (+/+: myd/myd), respectively.
doi:10.1371/journal.pone.0106721.g006

muscle contractions. However, such presumable membrane fragility may be protected in part by the dysferlin functions.

It is known that dysferlin plays a role in membrane repair pathway and several proteins are known to interact with dysferlin, suggesting that dysferlin forms a protein complex during the membrane repair process. MG53 has been shown to interact with dysferlin and participate in membrane repair, and genetic disruption of MG53 in mice results in muscular dystrophy [22]. Caveolin-3 is known to interact with dysferlin and MG53 [31,35]. In the present study, however, we did not observe compensatory upregulation of these proteins in *fukutin*$^{Hp/-}$ mice, suggesting that dysferlin functions other than membrane repair may play protective roles in the *fukutin*$^{Hp/-}$ mice. Recently, accumulating evidence has suggested new dysferlin roles other than membrane repair, such as T-tubule formation, maintenance, and stabilizing stress-induced Ca^{2+} signaling [36,37]. In addition, it has been reported that dysferlin deficiency leads to increased expression of complement factors and that complement-mediated muscle injury is associated with the pathogenesis of dysferlin-deficient muscular dystrophy [38]. Therefore, it is possible that such impairments independently or synergically contribute to the pathology of the double mutant mice.

Our results showed, rather unexpectedly, that the double-mutant (*dysferlin*$^{sjl/sjl}$: *Large*$^{myd/myd}$) mice did not exhibit significant deterioration of muscle pathology compared with the single-mutant (*dysferlin*$^{sjl/+}$: *Large*$^{myd/myd}$) mice. These data suggest that the protective effects of dysferlin in *Large*$^{myd/myd}$ mice were slightly or much reduced compared with those in *fukutin*$^{Hp/-}$ mice. Since *Large*$^{myd/myd}$ mice showed severe and rapid progressive pathology while *fukutin*$^{Hp/-}$ mice were asymptomatic, our data suggest that the protective effect of dysferlin may be less when disease pathology is advanced and/or severe. It has been reported that a double mutant of dysferlin and dystrophin produced a more exacerbated phenotype than did either single mutant [39]. In our colony, *Large*$^{myd/myd}$ mice show much more severe and rapid progressive pathology than do dystrophin-deficient mdx mice, supporting our hypothesis of a limited protective effect of dysferlin in dystrophic pathology. Interestingly, the (*dysferlin*$^{sjl/sjl}$: *Large*$^{myd/myd}$) mice, however, showed a significantly worse phenotype that did the (*dysferlin*$^{+/+}$: *Large*$^{myd/myd}$) mice. In addition, there is a tendency toward a worse phenotype in the order of dysferlin amount, *i.e.* (*dysferlin*$^{+/+}$: *Large*$^{myd/myd}$), (*dysferlin*$^{sjl/+}$: *Large*$^{myd/myd}$), and (*dysferlin*$^{sjl/sjl}$: *Large*$^{myd/myd}$). These data support the possibility that the protective effect of dysferlin is present even in the severe dystrophic *Large*$^{myd/myd}$ mice. We conclude that dysferlin has the potential to protect muscular dystrophy progression; however, its effect may depend on disease severity and the amount/activity of dysferlin proteins.

Recently, we showed that the retrotransposal insertion in the 3′-UTR region of *fukutin* causes abnormal mRNA splicing, which is induced by a strong splice acceptor site in SVA and a rare alternative donor site in the last exon, to produce an aberrantly spliced fukutin protein [7]. The introduction of antisense oligonucleotides that target the splice acceptor, the predicted exonic splicing enhancer, and the intronic splicing enhancer prevented the pathogenic exon trapping by SVA in the cells of FCMD patients as well as model mice (*fukutin*$^{Hp/Hp}$ and *fukutin*$^{Hp/-}$) [7]. This therapeutic strategy can potentially be applied to almost all FCMD patients in Japan, and can therefore be the first radical clinical treatment for dystroglycanopathies. However, there was no animal model to test the effectiveness of the antisense oligonucleotide therapy. Since *fukutin*$^{Hp/-}$ mice do not exhibit any signs of muscular dystrophy [23], they are not a great model for examining therapeutic effects of this strategy. Skeletal muscle-selective fukutin cKO mice, MCK-fukutin-cKO and Myf5-fukutin-cKO, showed dystrophic pathology [24], but they do not possess the retrotransposal insertion, and thus they are not applicable for testing the antisense oligonucleotide therapy. Our present study demonstrates more severe dystrophic phenotype of (*dysferlin*$^{sjl/sjl}$: *fukutin*$^{Hp/-}$) mice compared with (*dysferlin*$^{sjl/sjl}$: *fukutin*$^{Hp/+}$) mice. Since the (*dysferlin*$^{sjl/sjl}$: *fukutin*$^{Hp/-}$) mice possess the retrotransposal insertion and show dystrophic phenotype, they will be used as the first model for evaluation of the antisense oligonucleotide therapy for FCMD. There is a possibility that the absence of dysferlin could add hurdles on how to interpret the results of the antisense oligonucleotide treatments; however, our quantitative assessments established in this study could overcome this issue. For example, macrophage infiltration (Fig. 4B), connective tissue infiltration (Fig. 4D), and membrane fragility in quadriceps muscles (Fig. 5B) were significantly increased only in the (*dysferlin*$^{sjl/sjl}$: *fukutin*$^{Hp/-}$) mice. These parameters in the (*dysferlin*$^{sjl/sjl}$: *fukutin*$^{Hp/+}$) mice were not changed compared with those in the (*dysferlin*$^{sjl/+}$: *fukutin*$^{Hp/+}$) and the (*dysferlin*$^{sjl/+}$: *fukutin*$^{Hp/-}$) mice, and therefore can be used for quantitative evaluation for therapeutic effects of the antisense oligonucleotide treatments. We hope that generation of this novel FCMD model and establishment of the quantitative evaluation for disease severity will accelerate the future translational researches to overcome FCMD.

Supporting Information

Figure S1 Expression of dysferlin and dysferlin-interacting proteins in *fukutin*$^{Hp/-}$ mice. (A) Western blot analysis of dysferlin, caveolin-3, and MG53 in skeletal muscle extracts from fukutin-deficient *fukutin*$^{Hp/-}$ (Hp/−), and control *fukutin*$^{Hp/+}$ (Hp/+) mice. A representative two individual samples for each mouse line are shown in the blots. (B) Quantification of protein expression (panel A) was shown in graphs. Data shown are the average with standard deviations ($n = 4$ for dysferlin, $n = 3$ for caveolin-3 and MG53). (C) Immunofluorescence analysis of dysferlin in *fukutin*$^{Hp/-}$ (Hp/−) and *fukutin*$^{Hp/+}$ (Hp/+) mice. Bar, 50 μm.
(DOCX)

Acknowledgments

We would like to thank past and present members of the Dr. Toda's laboratory for fruitful discussions and scientific contributions. We also thank Dr. Jennifer Logan for help in editing the manuscript.

Author Contributions

Conceived and designed the experiments: MK ZL TT. Performed the experiments: MK ZL CI KM. Analyzed the data: MK CI. Contributed reagents/materials/analysis tools: CM KM. Contributed to the writing of the manuscript: MK TT.

References

1. Davies KE, Nowak KJ (2006) Molecular mechanisms of muscular dystrophies: old and new players. Nat Rev Mol Cell Biol 7: 762–773.
2. Barresi R, Campbell KP (2006) Dystroglycan: from biosynthesis to pathogenesis of human disease. J Cell Sci 119: 199–207.
3. Michele DE, Barresi R, Kanagawa M, Saito F, Cohn RD, et al. (2002) Post-translational disruption of dystroglycan-ligand interactions in congenital muscular dystrophies. Nature 418: 417–422.
4. Yoshida-Moriguchi T, Yu L, Stalnaker SH, Davis S, Kunz S, et al. (2010) O-mannosyl phosphorylation of alpha-dystroglycan is required for laminin binding. Science 327: 88–92.
5. Fukuyama Y, Osawa M, Suzuki H (1981) Congenital progressive muscular dystrophy of the Fukuyama type - clinical, genetic and pathological considerations. Brain Dev 3: 1–29.
6. Kobayashi K, Nakahori Y, Miyake M, Matsumura K, Kondo-Iida E, et al. (1998) An ancient retrotransposal insertion causes Fukuyama-type congenital muscular dystrophy. Nature 394: 388–392.
7. Taniguchi-Ikeda M, Kobayashi K, Kanagawa M, Yu CC, Mori K, et al. (2011) Pathogenic exon-trapping by SVA retrotransposon and rescue in Fukuyama muscular dystrophy. Nature 478: 127–131.
8. Godfrey C, Clement E, Mein R, Brockington M, Smith J, et al. (2007) Refining genotype phenotype correlations in muscular dystrophies with defective glycosylation of dystroglycan. Brain 130: 2725–2735.
9. Wells L (2013) The O-Mannosylation Pathway: Glycosyltransferases and Proteins Implicated in Congenital Muscular Dystrophy. J Biol Chem 288: 6930–6935.
10. Vuillaumier-Barrot S, Bouchet-Séraphin C, Chelbi M, Devisme L, Quentin S, et al. (2012) Identification of mutations in TMEM5 and ISPD as a cause of severe cobblestone lissencephaly. Am J Hum Genet 91: 1135–1143.
11. Jae LT, Raaben M, Riemersma M, van Beusekom E, Blomen VA, et al. (2013) Deciphering the glycosylome of dystroglycanopathies using haploid screens for lassa virus entry. Science 340: 479–483.
12. Buysse K, Riemersma M, Powell G, van Reeuwijk J, Chitayat D, et al. (2013) Missense mutations in β-1,3-N-acetylglucosaminyltransferase 1 (B3GNT1) cause Walker-Warburg syndrome. Hum Mol Genet 22: 1746–1754.
13. Stevens E, Carss KJ, Cirak S, Foley AR, Torelli S, et al. (2013) Mutations in B3GALNT2 cause congenital muscular dystrophy and hypoglycosylation of α-dystroglycan. Am J Hum Genet 92: 354–365.
14. Carss KJ, Stevens E, Foley AR, Cirak S, Riemersma M, et al. (2013) Mutations in GDP-mannose pyrophosphorylase B cause congenital and limb-girdle muscular dystrophies associated with hypoglycosylation of α-dystroglycan. Am J Hum Genet 93: 29–41.
15. Yoshida A, Kobayashi K, Manya H, Taniguchi K, Kano H, et al. (2001) Muscular dystrophy and neuronal migration disorder caused by mutations in a glycosyltransferase, POMGnT1. Dev Cell 1: 717–724.
16. Manya H, Chiba A, Yoshida A, Wang X, Chiba Y, et al. (2004) Demonstration of mammalian protein O-mannosyltransferase activity: coexpression of POMT1 and POMT2 required for enzymatic activity. Proc Natl Acad Sci USA 101: 500–505.
17. Inamori K, Yoshida-Moriguchi T, Hara Y, Anderson ME, Yu L, et al. (2012) Dystroglycan function requires xylosyl- and glucuronyltransferase activities of LARGE. Science 335: 93–96.
18. Yoshida-Moriguchi T, Willer T, Anderson ME, Venzke D, Whyte T, et al. (2013) SGK196 Is a Glycosylation-Specific O-Mannose Kinase Required for Dystroglycan Function. Science 341: 896–899.
19. Kuga A, Kanagawa M, Sudo A, Chan YM, Tajiri M, et al. (2012) Absence of post-phosphoryl modification in dystroglycanopathy mouse models and wild-type tissues expressing non-laminin binding form of α-dystroglycan. J Biol Chem 287: 9560–9567.
20. Mariano A, Henning A, Han R (2013) Dysferlin-deficient muscular dystrophy and innate immune activation. FEBS J 280: 4165–4176.
21. Bansal D, Miyake K, Vogel SS, Groh S, Chen CC, et al. (2003) Defective membrane repair in dysferlin-deficient muscular dystrophy. Nature 423: 168–172.
22. Cai C, Masumiya H, Weisleder N, Matsuda N, Nishi M, et al. (2009) MG53 nucleates assembly of cell membrane repair machinery. Nat Cell Biol 11: 56–64.
23. Kanagawa M, Nishimoto A, Chiyonobu T, Takeda S, Miyagoe-Suzuki Y, et al. (2009) Residual laminin-binding activity and enhanced dystroglycan glycosylation by LARGE in novel model mice to dystroglycanopathy. Hum Mol Genet 18: 621–631.
24. Kanagawa M, Yu CC, Ito C, Fukada S, Hozoji-Inada M, et al. (2013) Impaired viability of muscle precursor cells in muscular dystrophy with glycosylation defects and amelioration of its severe phenotype by limited gene expression. Hum Mol Genet 22: 3003–3015.
25. Bittner RE, Anderson LV, Burkhardt E, Bashir R, Vafiadaki E, et al. (1999) Dysferlin deletion in SJL mice (SJL-Dysf) defines a natural model for limb girdle muscular dystrophy 2B. Nat Genet 23: 141–142.
26. Kurahashi H, Taniguchi M, Meno C, Taniguchi Y, Takeda S, et al. (2005) Basement membrane fragility underlies embryonic lethality in fukutin-null mice. Neurobiol Dis 19: 208–217.
27. Grewal PK, Holzfeind PJ, Bittner RE, Hewitt JE (2001) Mutant glycosyltransferase and altered glycosylation of alpha-dystroglycan in the myodystrophy mouse. Nat Genet 28: 151–154.
28. Holzfeind PJ, Grewal PK, Reitsamer HA, Kechvar J, Lassmann H, et al. (2002) Skeletal, cardiac and tongue muscle pathology, defective retinal transmission, and neuronal migration defects in the Large(myd) mouse defines a natural model for glycosylation-deficient muscle-eye-brain disorders. Hum Mol Genet 11: 2673–2687.
29. Han R, Kanagawa M, Yoshida-Moriguchi T, Rader EP, Ng RA, et al. (2009) Basal lamina strengthens cell membrane integrity via the laminin G domain-binding motif of alpha-dystroglycan. Proc Natl Acad Sci USA 106: 12573–12579.
30. Straub V, Rafael JA, Chamberlain JS, Campbell KP (1997) Animal models for muscular dystrophy show different patterns of sarcolemmal disruption. J Cell Biol 139: 375–385.
31. Matsuda C, Hayashi YK, Ogawa M, Aoki M, Murayama K, et al. (2001) The sarcolemmal proteins dysferlin and caveolin-3 interact in skeletal muscle. Hum Mol Genet 10: 1761–1766.
32. Chan YM, Keramaris-Vrantsis E, Lidov HG, Norton JH, Zinchenko N, et al. (2010) Fukutin-related protein is essential for mouse muscle, brain and eye development and mutation recapitulates the wide clinical spectrums of dystroglycanopathies. Hum Mol Genet 19: 3995–4006.
33. Wang CH, Chan YM, Tang RH, Xiao B, Lu P, et al. (2011) Post-natal knockdown of fukutin-related protein expression in muscle by long-term RNA interference induces dystrophic pathology. Am J Pathol 178: 261–272.
34. Murakami T, Hayashi YK, Noguchi S, Ogawa M, Nonaka I, et al. (2006) Fukutin gene mutations cause dilated cardiomyopathy with minimal muscle weakness. Ann Neurol 60: 597–602.
35. Cai C, Weisleder N, Ko JK, Komazaki S, Sunada Y, et al. (2009) Membrane repair defects in muscular dystrophy are linked to altered interaction between MG53, caveolin-3, and dysferlin. J Biol Chem 284: 15894–15902.
36. Klinge L, Harris J, Sewry C, Charlton R, Anderson L, et al. (2010) Dysferlin associates with the developing T-tubule system in rodent and human skeletal muscle. Muscle Nerve 41: 166–173.
37. Kerr JP, Ziman AP, Mueller AL, Muriel JM, Kleinhans-Welte E, et al. (2013) Dysferlin stabilizes stress-induced Ca^{2+} signaling in the transverse tubule membrane. Proc Natl Acad Sci USA 110: 20831–20836.
38. Han R, Frett EM, Levy JR, Rader EP, Lueck JD, et al. (2010) Genetic ablation of complement C3 attenuates muscle pathology in dysferlin-deficient mice. J Clin Invest 120: 4366–4374.
39. Han R, Rader EP, Levy JR, Bansal D, Campbell KP (2011) Dystrophin deficiency exacerbates skeletal muscle pathology in dysferlin-null mice. Skelet Muscle 1: 35.

ORPHANET JOURNAL OF RARE DISEASES

RESEARCH Open Access

Japanese founder duplications/triplications involving *BHLHA9* are associated with split-hand/foot malformation with or without long bone deficiency and Gollop-Wolfgang complex

Eiko Nagata[1†], Hiroki Kano[2†], Fumiko Kato[1], Rie Yamaguchi[1], Shinichi Nakashima[1], Shinichiro Takayama[3], Rika Kosaki[4], Hidefumi Tonoki[5], Seiji Mizuno[6], Satoshi Watanabe[7], Koh-ichiro Yoshiura[7], Tomoki Kosho[8], Tomonobu Hasegawa[9], Mamori Kimizuka[10], Atsushi Suzuki[11], Kenji Shimizu[11], Hirofumi Ohashi[11], Nobuhiko Haga[12], Hironao Numabe[13], Emiko Horii[14], Toshiro Nagai[15], Hiroshi Yoshihashi[16], Gen Nishimura[17], Tatsushi Toda[18], Shuji Takada[19], Shigetoshi Yokoyama[19,22], Hiroshi Asahara[19,20], Shinichiro Sano[1,21], Maki Fukami[21], Shiro Ikegawa[2] and Tsutomu Ogata[1*]

Abstract

Background: Limb malformations are rare disorders with high genetic heterogeneity. Although multiple genes/loci have been identified in limb malformations, underlying genetic factors still remain to be determined in most patients.

Methods: This study consisted of 51 Japanese families with split-hand/foot malformation (SHFM), SHFM with long bone deficiency (SHFLD) usually affecting the tibia, or Gollop-Wolfgang complex (GWC) characterized by SHFM and femoral bifurcation. Genetic studies included genomewide array comparative genomic hybridization and exome sequencing, together with standard molecular analyses.

Results: We identified duplications/triplications of a 210,050 bp segment containing *BHLHA9* in 29 SHFM patients, 11 SHFLD patients, two GWC patients, and 22 clinically normal relatives from 27 of the 51 families examined, as well as in 2 of 1,000 Japanese controls. Families with SHFLD- and/or GWC-positive patients were more frequent in triplications than in duplications. The fusion point was identical in all the duplications/triplications and was associated with a 4 bp microhomology. There was no sequence homology around the two breakpoints, whereas rearrangement-associated motifs were abundant around one breakpoint. The rs3951819-*D17S1174* haplotype patterns were variable on the duplicated/triplicated segments. No discernible genetic alteration specific to patients was detected within or around *BHLHA9*, in the known causative SHFM genes, or in the exome.

(Continued on next page)

* Correspondence: tomogata@hama-med.ac.jp
†Equal contributors
[1]Department of Pediatrics, Hamamatsu University School of Medicine, Hamamatsu 431-3192, Japan
Full list of author information is available at the end of the article

(Continued from previous page)

Conclusions: These results indicate that *BHLHA9* overdosage constitutes the most frequent susceptibility factor, with a dosage effect, for a range of limb malformations at least in Japan. Notably, this is the first study revealing the underlying genetic factor for the development of GWC, and demonstrating the presence of triplications involving *BHLHA9*. It is inferred that a Japanese founder duplication was generated through a replication-based mechanism and underwent subsequent triplication and haplotype modification through recombination-based mechanisms, and that the duplications/triplications with various haplotypes were widely spread in Japan primarily via clinically normal carriers and identified via manifesting patients. Furthermore, genotype-phenotype analyses of patients reported in this study and the previous studies imply that clinical variability is ascribed to multiple factors including the size of duplications/triplications as a critical factor.

Keywords: *BHLHA9*, Split-hand/foot malformation, Long bone deficiency, Gollop-Wolfgang complex, Expressivity, Penetrance, Susceptibility, Japanese founder copy number gain

Introduction

Split-hand/foot malformation (SHFM), also known as ectrodactyly, is a rare limb malformation involving the central rays of the autopod [1,2]. It presents with median clefts of the hands and feet, aplasia/hypoplasia of the phalanges, metacarpals, and metatarsals, and syndactyly. SHFM results from failure to maintain the central portion of the apical ectodermal ridge (AER) in the developing autopod [1,2]. SHFM is divided into two forms: a non-syndromic form with limb-confined manifestations and a syndromic form with extra-limb manifestations [2]. Furthermore, non-syndromic SHFM can occur as an isolated abnormality confined to digits (hereafter, SHFM refers to this type) or in association with other limb abnormalities as observed in SHFM with long bone deficiency (SHFLD) usually affecting the tibia and in Gollop-Wolfgang complex (GWC) characterized by femoral bifurcation [1,2]. Both syndromic and non-syndromic forms are associated with wide expressivity and penetrance even among members of a single family and among limbs of a single patient [2].

SHFM and SHFLD are genetically heterogeneous conditions reviewed in ref. [2]. To date, SHFM has been identified in patients with heterozygous deletions or translocations involving the *DLX5–DLX6* locus at 7q21.2–21.3 (SHFM1) [3] (*DLX5* mutations have been detected recently), heterozygous duplications at 10q24 (SHFM3), heterozygous mutations of *TP63* at 3q27 (SHFM4), heterozygous deletions affecting *HOXD* cluster at 2q31 (SHFM5), and biallelic mutations of *WNT10B* at 12q31 (SHFM6); in addition, SHFM2 has been assigned to Xq26 by linkage analyses in a large Pakistani kindred [2]. Similarly, a genomewide linkage analysis in a large consanguineous family has identified two SHFLD susceptibility loci, one at 1q42.2–q43 (SHFLD1) and the other at 6q14.1 (SHFLD2); furthermore, after assignment of another SHFLD locus to 17p13.1–13.3 [4], duplications at 17p13.3 (SHFLD3) have been found in patients with SHFLD reviewed in ref. [2]. However, the GWC locus (loci) remains unknown at present.

The duplications at 17p13.3 identified to date are highly variable in size, and harbor *BHLHA9* as the sole gene within the smallest region of overlap [5-9]. *Bhlha9*/*bhlha9* is expressed in the limb bud mesenchyme underlying the AER in mouse and zebrafish embryos, and *bhlha9* knockdown has resulted in shortening of the pectoral fins in zebrafish [6]. Furthermore, *BHLHA9*-containing duplications have been identified not only in patients with SHFLD but also in those with SHFM and clinically normal family members [4-10]. These findings argue for a critical role of *BHLHA9* duplication in the development of SHFM and SHFLD, with variable expressivity and incomplete penetrance.

In this study, we report on *BHLHA9*-containing duplications/triplications with an identical fusion point and various haplotype patterns that were associated with a range of limb malformations including GWC, and discuss on characteristic clinical findings, genomic basis of Japanese founder copy number gains, and underlying factors for phenotypic variability.

Materials and methods

Patients/subjects

We studied 68 patients with SHFM (n = 55), SHFLD (n = 11), or GWC (n = 2), as well as 60 clinically normal relatives, from 51 Japanese families; the pedigrees of 27 of the 51 families and representative clinical findings are shown in Figure 1. All the probands 1–51 had a normal karyotype. Southern blot analysis for SHFM3 locus had been performed in 28 probands with SHFM, indicating 10q24 duplications in two of them [11]. Clinical features including photographs and roentgenograms of a proband with GWC and his brother with SHFLD (family 23 in Figure 1A) were as described previously [12]. The residencies of families 1–51 were widely distributed throughout Japan.

Ethical approval and samples

This study was approved by the Institutional Review Board Committees of Hamamatsu University School of

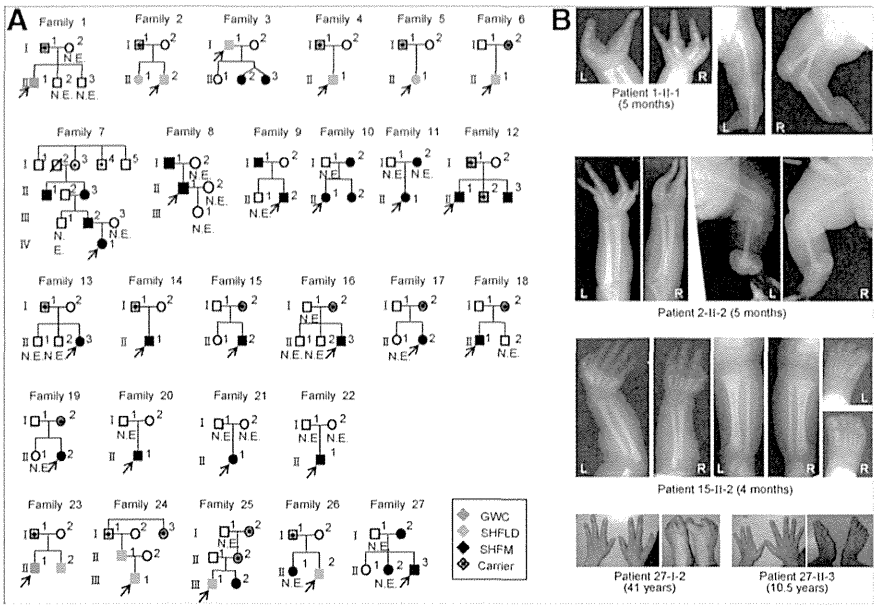

Figure 1 Clinical summary. A. Pedigrees of 27 Japanese families with duplications (families 1–22) and triplications (families 23–27) of a ~200 kb region involving *BHLHA9*. The duplications/triplications are associated with GWC, SHFLD, SHFM, or normal phenotype (carriers). N.E.: Not examined molecularly. **B**. Representative clinical findings. Each patient is indicated by a family-generation-individual style and corresponds to the patient/subject shown in Figure 1A and Additional file 5. The top panel: GWC with right bifid femur; the second panel: SHFLD with bilateral tibial deficiencies, the third panel: SHFM with polydactyly; and the bottom panel: SHFM.

Medicine, RIKEN, and National Center for Child Health and Development, and was performed using peripheral leukocyte samples after obtaining written informed consent for the molecular analysis and the publication of genetic and clinical data after removing information for personal identification (e.g., name, birthday, and facial photograph) from the adult subjects (^{3} 20 years) or from the parents of the child subjects (below 20 years). Furthermore, informed assent was also obtained from child subjects between 6–20 years.

Samples and primers

The primers utilized in this study are summarized in Additional file 1.

Molecular studies

Sanger sequencing, fluorescence *in situ* hybridization (FISH), microsatellite genotyping, Southern blotting, and bisulfite sequencing-based methylation analysis were performed by the standard methods, as reported previously [13]. Quantitative real-time PCR (qPCR) analysis was carried out by the SYBR Green methods on StepOnePlus system, using *RNaseP* as an internal control (Life Technologies). Genomewide oligonucleotide-based array comparative genomic hybridization (CGH) was performed with a catalog human array (4 × 180 K format, ID G4449A) according to the manufacturer's instructions (Agilent Technologies), and obtained copy number variants/polymorphisms were screened with Agilent Genomic Workbench software using the Database of Genomic Variants (http://dgv.tcag.ca/dgv/app/home). Sequencing of a long region encompassing *BHLHA9* was performed with the Nextera XT kit on MiSeq (Illumina), using SAMtools v0.1.17 software (http://samtools.sourceforge.net/). Exome sequencing was performed as described previously [14].

Assessment of genomic environments around the fusion points

Repeat elements around the fusion point were searched for using Repeatmasker (http://www.repeatmasker.org). Rearrangement-inducing DNA features were investigated for 300 bp regions at both the proximal and the distal sides of each breakpoint, using GEECEE (http://emboss.bioinformatics.nl/cgi-bin/emboss/geecee) for calculation of the average GC content, PALINDROME (http://mobyle.pasteur.fr/cgi-bin/portal.py#forms::palindrome) and Non-B DB (http://nonb.abcc.ncifcrf.gov) for the examination of the palindromes and non-B (non-canonical) structures, and Fuzznuc (http://emboss.bioinformatics.nl/cgi-bin/emboss/fuzznuc) for the assessment of rearrangement-associated sequence motifs and tri/tetranucleotides [15-20]. For controls, we examined 48 regions of 600 bp long selected at an interval of 1.5 Mb from the entire chromosome 17.

Statistical analysis

The statistical significance of the frequency was analyzed by the two-sided Fisher's exact probability test.

Results

Sequence analysis of the known causative/candidate genes

We performed direct sequencing for the previously known causative genes (*DLX5*, *TP63*, and *WNT10B*) reviewed in ref. [2] in the probands 1–51. Although no pathologic mutation was identified in *DLX5* and *TP63*, the previously reported homozygous missense mutation of *WNT10B* (c.944C > T, p.R332W) [21] was detected in the proband 48 with SHFM who was born to healthy consanguineous parents heterozygous for this mutation. In addition, while no variation was detected in *DLX5* and *WNT10B*, rs34201045 (4 bp insertion polymorphism) in *TP63* [21] was detected with an allele frequency of 61%.

We also examined *BHLHA9*, because gain-of-function mutations of *BHLHA9* as well as *BHLHA9*-harboring duplications may lead to limb malformations. No sequence variation was identified in the 51 probands.

Array CGH analysis

Array CGH analysis was performed for the probands 1–51, showing increased copy numbers at 17p13.3 encompassing *BHLHA9* (SHFLD3) in the probands 1–27 from families 1–27 (Figure 1A). Furthermore, heterozygous duplications at 10q24 (SHFM3) were detected in the probands 49–51, i.e., a hitherto unreported patient with paternally inherited SHFM (his father also had the duplication) and the two patients who had been indicated to have the duplications by Southern blot analysis [11]. No copy number alteration was observed at other SHFM/SHFLD loci in the probands 1–27 and 49–51. In the remaining probands 28–48, there was no copy number variation that was not registered in the Database of Genomic Variants.

Identical fusion points in *BHLHA9*-containing duplications/triplications

The array CGH indicated that the increased copy number regions at 17p13.3 were quite similar in the physical size in the probands 1–27 and present in three copies in the probands 1–22 and in four copies in the probands 23–27 (Figure 2A). Thus, FISH analysis was performed using 8,259 bp PCR products amplified from this region, showing two signals with a different intensity that was more obvious in the probands 23–27 (Figure 2A).

We next determined the fusion points of the duplications/triplications (Figure 2B). PCR products of 2,195 bp long were obtained with P1/P2 primers in the probands 1–27, and the fusion point was determined by direct sequencing for 418 bp PCR products obtained with P3/P4 primers. The fusion point was identical in all the probands 1–27; it resided on intron 1 of *ABR* and intron 1 of *YWHAE*, and was associated with a 4 bp microhomology.

Then, we performed qPCR analysis for a 214 bp region harboring the fusion point, using P5/P6 primers (Figure 2C and Additional file 2). The fusion point was present in a single copy in the probands 1–22 and in two copies in the probands 23–27. The results showed that the identical genomic segment harboring *BHLHA9* was tandemly duplicated in the probands 1–22 and triplicated in the probands 23–27. According to GRCh37/hg19 (http://genome.ucsc.edu/), the genomic segment was 210,050 bp long.

We also performed array CGH and qPCR for the fusion point in 15 patients other than the probands and 47 clinically normal relatives from the 27 families (Figures 1 and 2C). The duplications/triplications were identified in all the 15 patients. Thus, in a total of 42 patients, duplications/triplications were found in 29 SHFM patients, 11 SHFLD patients, and two GWC patients. Furthermore, the duplications/triplications were also present in 22 of the 47 clinically normal relatives. In particular, they were invariably identified in either of the clinically normal parents when both of them were examined; they were also present in other clinically normal relatives in families 7, 12, 24, and 25.

Since the above data indicated the presence of duplications/triplications in clinically normal subjects, we performed qPCR for the fusion point in 1,000 Japanese controls. The fusion point was detected in a single copy in two subjects (Subjects 1 and 2 in Figure 2C). We also performed array CGH in 200 of the 1,000 controls including the two subjects, confirming the duplications in the two subjects and lack of other copy number variations, including deletions involving *BHLHA9*, which were not registered in the Database of Genomic Variants in the 200 control subjects. The frequency of duplications/triplications was significantly higher in the probands than in the control subjects (27/51 vs. 2/1,000, $P = 3.5 \times 10^{-37}$).

Various haplotype patterns on the duplicated/triplicated segments

We carried out genotyping for rs3951819 (A/G SNP on *BHLHA9*) and *D17S1174* (CA repeat microsatellite locus) on the genomic segment subjected to duplications/triplications (Figure 2A), and determined rs3951819-*D17S1174* haplotype patterns. Representative results are shown in Figure 2D, and all the data are available on request. Various haplotype patterns were identified on the single, the duplicated, and the triplicated segments, and the [A-14] haplotype was most prevalent on the duplicated/triplicated segments (Table 1). While the distribution of CA repeat lengths on the single segments was discontinuous, similar discontinuous distribution was

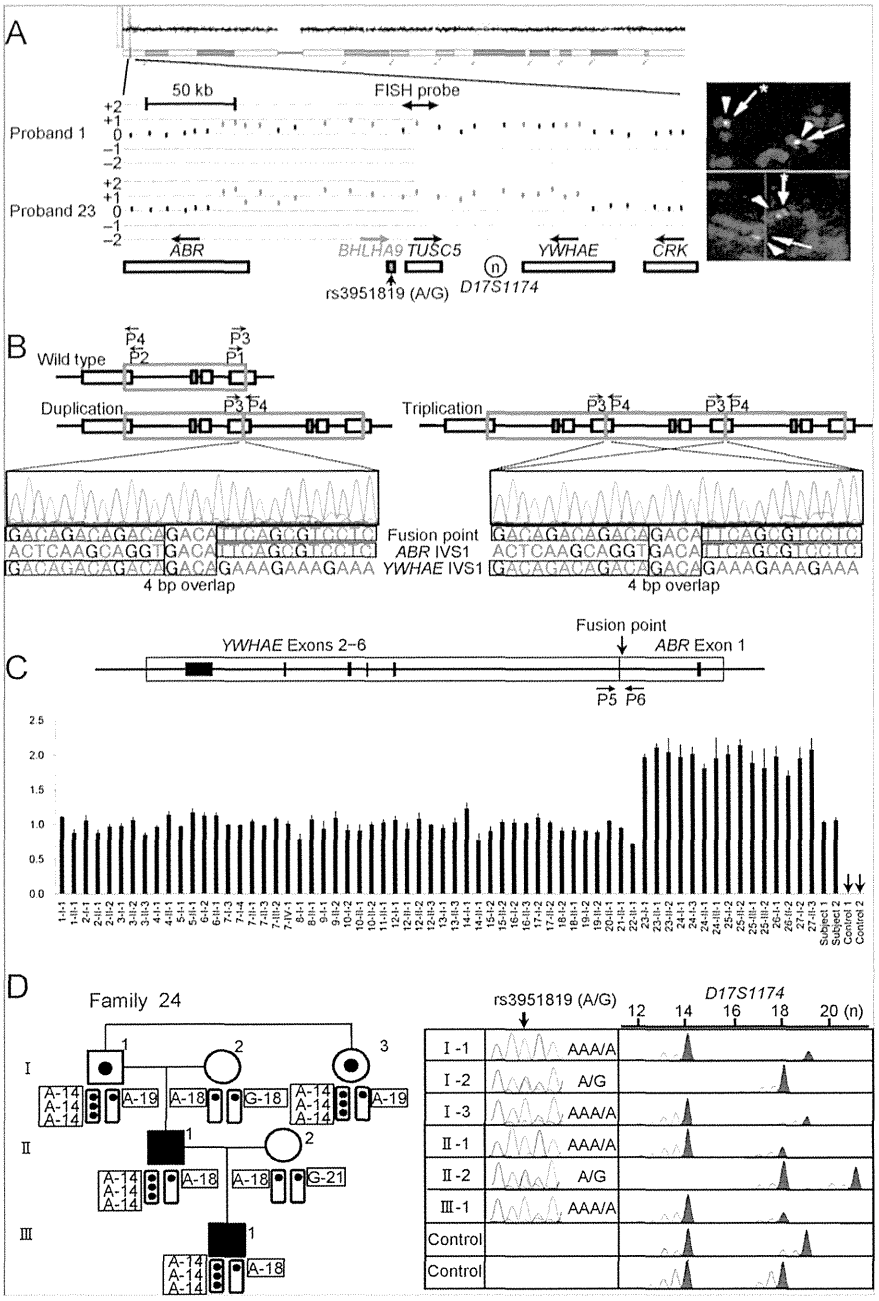

Figure 2 (See legend on next page.)

(See figure on previous page.)
Figure 2 Identification and characterization of the duplications/triplications involving *BHLHA9* at chromosome 17p13.3. A. Array CGH and FISH analyses in proband 1 and proband 23 with GWC. In array CGH analysis, the black and the red dots denote the normal and the increased copy numbers, respectively. Since the log2 signal ratios for a ~200 kb region encompassing *BHLHA9* are around +0.5 in the proband 1 and around +1.0 in the proband 23, this indicates the presence of three and four copies of this region in the two probands, respectively. In FISH analysis, two red signals with an apparently different density are detected by the 8,289 bp PCR probe (the stronger signals are indicated with asterisks). The green signals derive from an internal control probe (CEP17). The arrows on the genes show transcriptional directions. Rs3951819 (A/G) resides within *BHLHA9*. **B**. Determination of the fusion point. The fusion has occurred between intron 1 of *ABR* and intron 1 of *YWHAE*, and is associated with a 4 bp (GACA) microhomology. P1–P4 show the position of primers. **C**. Quantitative real-time PCR analysis. The upper part denotes the fusion point. P5 & P6 show the position of primers. The lower part shows the copy number of the fusion point in patients/subjects with duplications/triplications (indicated by a family-generation-individual style corresponding to that in Figure 1 and Additional file 5). Subject-1 and subject-2 denote the two control subjects with the duplication, and control-1 and control-2 represent normal subjects without the duplication/triplication. **D**. The rs3951819 (A/G SNP)–*D17S1174* (CA repeat number) haplotype patterns in family 24. Assuming no recombination between rs3951819 and *D17S1174*, the haplotype patterns of the family members are determined as shown here. The haplotype patterns of the remaining families have been interpreted similarly.

also observed in the Japanese general population (see Additional file 3).

Genomic environments around the breakpoints

The breakpoint on *YWHAE* intron 1 resided on a simple *Alu* repeat sequence, and that on *ABR* intron 1 was present on a non-repetitive sequence. There was no low copy repeat around the breakpoints. Comparison of the frequencies of known rearrangement-inducing DNA features between 600 bp sequences around the breakpoints and those of 48 regions selected at an interval of 1.5 Mb from chromosome 17 revealed that palindromes, several types of non-B DNA structures, and a rearrangement-associated sequence motif were abundant around the breakpoint on *YWHAE* intron 1 (see Additional file 4).

Clinical findings of families 1–27

Clinical assessment revealed several notable findings. First, duplications/triplications were associated with SHFM, SHFLD, GWC, or normal phenotype, with inter- and intra-familial clinical variability (Figure 1A). Second, in the 42 patients, split hand (SH) was more prevalent than split foot (SF) (41/42 vs. 17/42, $P = 6.2 \times 10^{-9}$), and long bone defect (LBD) was confined to lower extremities (0/42 vs. 13/42, $P = 4.1 \times 10^{-5}$) (Table 2 and Additional file 5). Third, there was no significant sex difference in the ratio between patients with limb malformations and patients/carriers with duplications/triplications (26/38 in males vs. 16/26 in females, $P = 0.60$) (Table 2 and Additional file 5). Fourth, the ratio of LBD positive families was significantly higher in triplications than in duplications (4/5 vs. 16/22, $P = 0.047$) (Figure 1A and Table 2). Fifth, while the duplications/triplications were transmitted from patients to patients, from carriers to patients, and from a carrier to a carrier (from I-1 to II-2 in family 12), transmission from a patient to a carrier was not identified (Figure 1A); it should be pointed out, however, that molecular analysis in a clinically normal child born to an affected parent was possible only in a single adult subject (II-1 in family 27), and that molecular analysis in clinically

Table 1 The rs3951819 (A/G SNP) – *D17S1174* (CA repeat number) haplotype

Patterns of the 210,050 bp segment subjected to copy number gains	
Haplotype pattern	**Family**
<Single segment>	
[A-14]	1, 5, 9, 15, 17, 19, 23, 26
[A-16]	12
[A-18]	3, 14, 15, 24, 25, 26
[A-19]	2, 6, 13, 19, 20, 24, 25, 27
[A-21]	5, 23
[G-12]	17
[G-14]	2, 3, 6, 12, 13, 19, 26
[G-18]	3, 5, 17, 18, 24, 25
[G-19]	9, 12, 18, 20, 25
[G-21]	1, 9, 19, 24, 27
[A-14] or [G-14]	16
[A-18] or [G-18]	4
[A-19] or [G-19]	4
[A-21] or [G-21]	16
<Duplicated segments>	
[A-14] + [A-14]	5, 12, 13, 14, 15, 20
[A-14] + [A-18]	1
[A-14] + [G-18] or [G-14] + [A-18]	2, 3, 4, 6, 9, 16, 17
[A-14] + [G-18] or [A-14] + [G-19]	18
[A-14] + [G-14] or [G-14] + [G-14]	19
<Triplicated segments>	
[A-14] + [A-14] + [A-14]	23, 24
[A-14] + [A-14] + [G-14]	25
[A-14] + [A-19] + [A-19]	26
[A-14] + [G-18] + [G-18] or [G-14] + [A-18] + [G-18]	27

The haplotype patterns written in the left column have been detected in at least one patient/subject in the families described in the right column.
Genotyping could not be performed in several patients/subjects who had been repeatedly examined previously, because of the extremely small amount of DNA samples that were virtually used up in the sequencing and array CGH analyses.

Table 2 Summary of clinical findings in patients/carriers with duplications/triplications involving *BHLHA9*

	SHFM (+) patients			LBD (+) patients			Patient ratio*			LBD (+) families		
	SH	SF	*P*-value	U-LBD	L-LBD	*P*-value	Male	Female	*P*-value	Trip	Dup	*P*-value
This study	41/42	17/42	6.2×10^{-9}	0/42	13/42	4.1×10^{-5}	26/38	16/26	0.60	4/5	16/22	0.047
Previous studies	63/84	23/84	8.6×10^{-10}	11/91	42/91	5.7×10^{-7}	68/114	31/79	5.7×10^{-3}	...	...	...
Sum	104/126	40/126	1.1×10^{-16}	11/133	55/133	3.0×10^{-10}	94/152	47/105	7.6×10^{-3}	...	...	...

SHFM: split-hand/foot malformation; SH: split hand; SF: split foot; LBD: long bone deficiency; U: upper; L: lower; Trip: triplication; and Dup: duplication.
In the previous studies, patients without detailed phenotypic description and those of unknown sex have been excluded (3–9).
*The ratio between patients with limb malformations and patients/carriers with duplications/triplications, i.e. the number of patients over the number of patients plus carriers.

normal children <20 years old was possible only in two subjects (II-2 in family 12 and II-1 in family 15). Lastly, limb malformation was inherited in an apparently autosomal dominant manner (from patients to patients), or took place as an apparently *de novo* event or as an apparently autosomal recessive trait (from clinically normal parents to a single or two affected children) (Figure 1A).

Attempts to identify a possible modifier(s)

The variable expressivity and incomplete penetrance in families 1–27 suggest the presence of a possible modifier (s) for the development of limb malformations. Thus, we performed further molecular studies in patients/subjects in whom DNA samples were still available, and compared the molecular data between patients with SHFM and those with SHFLD for the assessment of variable expressivity and between SHFM, SHFLD, or total patients and carriers for the evaluation of incomplete penetrance.

We first examined the possibility that the modifier(s) resides within or around *BHLHA9* (see Additional file 6). There was no *BHLHA9* mutation in all the 21 examined probands with SHFM, SHFLD, or GWC, as described in the section of "Sequence analysis of the known causative/candidate genes". The rs3951819 A/G SNP pattern on the duplicated/triplicated segments was apparently identical between patients and carriers (e.g. Figure 2D), and the frequency of A/G allele on the normal chromosome 17 was similar between SHFM and SHFLD patients and between SHFM, SHFLD, or total patients and carriers (see Additional file 7). The results of other known SNPs on *BHLHA9* (rs185242872, rs18936498, and rs140504068) were not informative, because of absence or extreme rarity of minor alleles. Furthermore, in SHFM families 7, 12, and 18, sequencing of a 7,406 bp region encompassing *BHLHA9* and Southern blot analysis using five probes and *Mfe*I-, *Ssp*I-, and *Sac*I-digested genomic DNA revealed no variation specific to the patients, and methylation analysis for a CpG rich region at the upstream of *BHLHA9* delineated massive hypomethylation in all the patients/carriers examined.

Next, we examined the possibility that a variant(s) of known causative genes constitutes the modifier(s). Since rs34201045 in *TP63* was identified in the mutation analysis, we compared rs34201045 genotyping data between the 27 probands and the 15 carriers. The allele and genotype frequencies were similar between SHFM and SHFLD patients and between SHFM, SHFLD, or total patients and carriers (see Additional file 8).

We finally performed exome sequencing in SHFM families 13 and 17–19. However, there was no variation specific to the patients. In addition, re-examination of the genomewide array CGH data showed no discernible copy number variation specific to the patients.

Discussion

BHLHA9 overdosage and clinical characteristics

We identified duplications/triplications of a ~ 200 kb genomic segment involving *BHLHA9* at 17p13.3 in 27 of 51 families with SHFM, SHFLD, or GWC. To our knowledge, this is the first study revealing the underlying genetic factor for the development of GWC, and demonstrating the presence of triplications involving *BHLHA9* that were suggested but not confirmed in the previous studies [5,9]. Furthermore, this study indicates that *BHLHA9*-containing duplications/triplications are the most frequent underlying factor for the development of limb malformations at least in Japan. Notably, SHFLD and GWC with LBD were significantly more frequent in patients with triplications than in those with duplications, and the duplications/triplications were identified in clinically normal familial members and in the general population. These findings imply that increased *BHLHA9* copy number constitutes a strong susceptibility, rather than a causative, factor with a dosage effect for the development of a range of limb malformations. Since *Bhlha9* is expressed in the developing ectoderm adjacent to the AER rather than the AER itself in mouse embryos [6], *BHLHA9* appears to play a critical role in the limb development by interacting with the AER. While the duplications/triplications identified in this study included *TUSC5* and generated an *ABR-YWHAE* chimeric gene (Figure 2C), *TUSC5* duplication and the chimeric gene formation are not common findings in the previously reported patients with duplications at 17p13.3 and SHFM and/or SHFLD [5-9]. In addition, none of *Tusc5*, *Abr*, and *Ywhae* is specifically expressed in the developing mouse limb buds [22] (A Transcriptome Atlas Database

for Mouse Embryo of Eurexpress Project, http://www.eurexpress.org/ee/project/).

Several clinical findings are noteworthy in patients/subjects with duplications/triplications. First, SH was more frequent than SF in this study as well as in the previous studies, and LBD was confined to lower extremities in this study and was more frequent in lower extremities than in upper extremities in the previous studies (Table 2) [4-10]. This implies that *BHLHA9* overdosage exerts differential effects on the different parts of limbs. Second, while limb malformations were similarly identified between males and females in this study, they were more frequently observed in males than in females in the previous studies (Table 2) [4-10]. In this regard, it has been reported that testosterone influences the digital growth pattern as indicated by the lower second to fourth digit length ratio in males than in females [23-25], and that Caucasian males have higher serum testosterone values and lower second to fourth digit length ratios than Oriental males [26,27]. Such testosterone effects on the digital growth pattern with ethnic difference may explain why male dominant manifestation was observed in the previous studies primarily from Caucasian countries and was not found in this study. Lastly, LBD was more prevalent in patients with triplications than in those with duplications. This suggests that LBD primarily occurs when the effects of *BHLHA9* overdosage are considerably elevated.

Genomic basis of the Japanese founder copy number gains

The duplications/triplications were associated with the same fusion point and variable haplotype patterns. Since there was no sequence homology or low-copy repeats around the breakpoints, it is unlikely that such duplications/triplications were recurrently produced in different individuals by non-allelic homologous recombination (NAHR) [17,20]. Instead, it is assumed that a Japanese founder duplication took place in a single ancestor, and was spread with subsequent triplication and modification of the haplotype patterns.

The most likely genomic basis of the Japanese duplications/triplications is illustrated in Additional file 9. Notably, a 4 bp (GACA) microhomology was identified at the duplication fusion point (Figure 2B). A microhomology refers to two to five nucleotides common to the sequences of the two breakpoints, and is found as an overlapping sequence at the join point [16,19,20]. This suggests that the Japanese founder duplication was generated by replication-based mechanisms such as fork stalling and template switching (FoSTeS) and microhomology-mediated break-induced replication (MMBIR), because the presence of such a microhomology is characteristic of FoSTeS/MMBIR [17-20]. Indeed, such a simple tandem duplication with a microhomology can be produced by one time FoSTeS/MMBIR [17-20], although it could also be generated by non-homologous end-joining (NHEJ) [17]. Since the [A-14] haplotype was most prevalent on the duplicated/triplicated segments, it is inferred that a genomic rearrangement occurred in an ancestor with the [A-14] haplotype, yielding the founder duplication with the [A-14] + [A-14] haplotype. Furthermore, the presence of multiple stimulants for genomic rearrangements around the breakpoint on *YWHAE* intron 1 would have facilitated the generation of the founder duplication. In particular, non-B structures are known to stimulate the occurrence of both replication-based FoSTeS/MMBIR and double-strand breaks and resultant NHEJ [17,28,29], although the relative importance of each non-B DNA structure is largely unknown.

Subsequent triplication and haplotype modification can develop from the Japanese founder duplication through unequal interchromatid and interchromosomal recombinations [17,20]. Indeed, a tandem triplication with the [A-14] + [A-14] + [A-14] haplotype can be generated by unequal exchange between sister chromatids with the [A-14] + [A-14] haplotype, and various haplotype patterns are yielded by unequal interchromosomal exchanges involving the duplicated or triplicated segments. Furthermore, the haplotype variation would be facilitated by unequal exchanges between sister chromatids harboring duplications/triplications with various haplotype patterns and by the further unequal interchromosomal exchanges.

Underlying factors for the phenotypic variability

The duplications/triplications were accompanied by limb malformations with variable expressivity and incomplete penetrance. Although this may suggest the presence of a possible modifier(s) for the development of limb malformations, such a modifier(s) was not detected. In particular, while patient-to-carrier transmission of duplications/triplications was not identified in this study, even patient-to-carrier-to-patient transmission has been reported in three pedigrees [5,6,10]. Such transmission pattern with incomplete penetrance characterized by skipping of a generation is apparently inexplicable by assuming a modifier (s) interacting with *BHLHA9* or independent of *BHLHA9* on the duplication/triplication positive chromosome 17, on the normal chromosome 17, or on other chromosomes (Figure 3, Models A, B, and C, see also the legends in Figure 3).

In this regard, it is noteworthy that the development of limb malformations is obviously dependent on the size of genomic segment subjected to copy number gains. Actually, limb malformation has occurred in only one of 21 large duplications encompassing *BHLHA9* (average 1.55 Mb, mean 1.12 Mb) and in 29 of 80 small duplications encompassing *BHLHA9* (average 244 kb, mean 263 kb) ($P = 5.9 \times 10^{-3}$) [8]. Consistent with this, the patients with large and

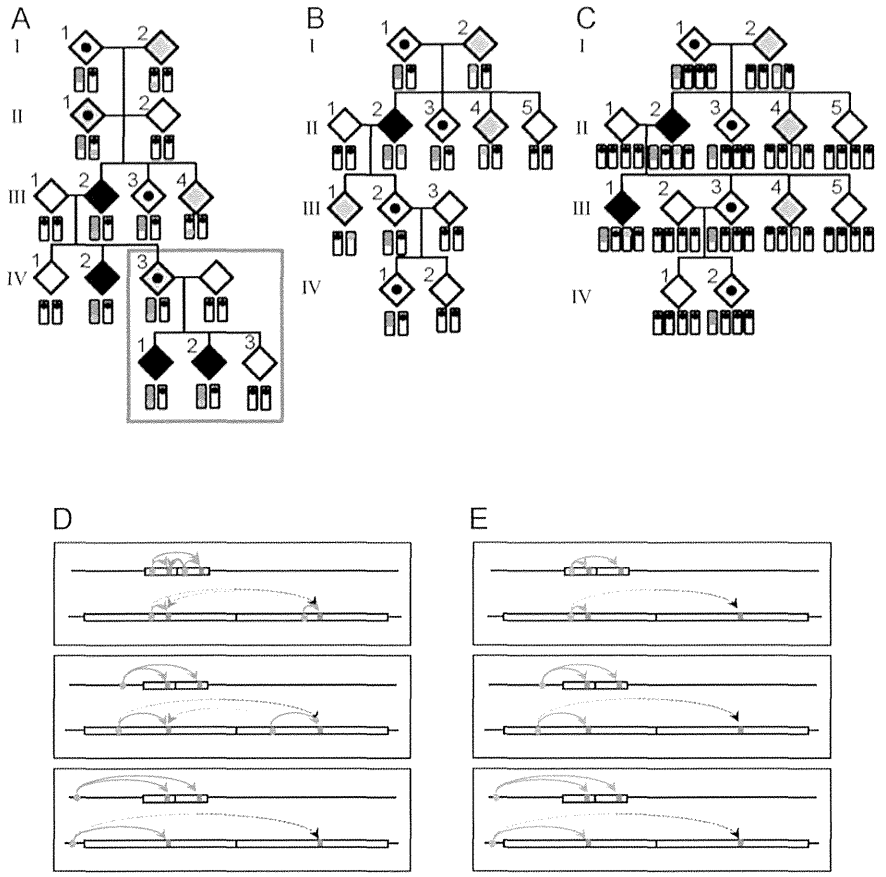

Figure 3 Models for a modifier(s) and effects of the duplication size. In models **A**–**C**, the yellow bars show chromosome 17, and the light green bars indicate other chromosomes. The two red dots represent the duplication at 17p13.3, and the blue dots indicate a putative modifier(s). Black painted diamonds represent limb malformation positive patients, dot-associated and gray painted diamonds indicate clinically normal carriers with the duplications and the modifier(s) respectively, and white painted diamonds denote clinically normal subjects without both the duplications and the modifier(s). **A**. This model assumes that co-existence of the duplication and a *cis*-acting modifier(s) causes limb malformation. If co-existence of the duplication and the *cis*-acting modifier(s) is associated with incomplete penetrance, this can explain all the transmission patterns observed to date, including the patient-to-carrier transmission and the presence of ≥ 2 affected children. **B**. This model postulates that the presence of a *cis*-acting modifier(s) on the normal chromosome 17 leads to limb malformation by enhancing the expression of the single *BHLHA9*, together with duplicated *BHLHA9* on the homologous chromosome. **C**. This model postulates that co-existence of the duplication at 17p13.3 and a modifier(s) on other chromosome causes limb malformation. In models **D**–**E**, the red bars represent *BHLHA9*, the blue circles indicate a physiological cis-regulatory element for *BHLHA9*, and the green circles indicate a non-physiological modifier(s) for *BHLHA9*. **D**. The physiological cis-regulatory element may be duplicated or non-duplicated, depending on its position relative to the size of the duplications. *BHLHA9* expression can be higher in small duplications than large duplications. **E**. The non-physiological modifier(s) can be transferred to various positions of the duplication positive chromosome 17, depending on the recombination places (see Model A). *BHLHA9* expression can be higher in small duplications than large duplications irrespective of the position of the modifier(s).

small duplications were ascertained primarily due to developmental retardation and limb malformation, respectively [8]. It is likely that a physiological cis-regulatory element for *BHLHA9* (e.g., an enhancer) can frequently but not invariably work on both of the duplicated *BHLHA9* when the duplication size is small but is usually incapable of working on duplicated *BHLHA9* when the duplication size is large, probably because of the difference in the chromatin structure (see Model D in Figure 3). Similar findings have also been reported in other genes. For example, small (~150 kb) and relatively small (600–800 kb) duplications involving a putative testis-specific enhancer(s) for *SOX9* have caused 46,XX testicular and ovotesticular disorders of sex development respectively, whereas large duplications (~2 Mb) involving the enhancer(s) have permitted normal ovarian development in 46,XX individuals [30].

Thus, a plausible explanation may be that a range of limb malformations emerge when the effects of *BHLHA9* overdosage exceed the threshold for the development of SHFM, SHFLD, or GWC, depending on the conditions of

other genetic and environmental factors including the size of duplications/triplications as an important but not definitive factor. One may argue that this notion is inconsistent with the apparent anticipation phenomenon that is suggested by the rare patient-to-carrier transmission and the frequent carrier-to-patient transmission of the duplications/triplications, because no specific factor(s) exaggerating the development of limb malformations is postulated in the next generation. However, the skewed transmission pattern would primarily be ascribed to ascertainment bias rather than anticipation [31]. Indeed, while clinically normal parents of disease positive children would frequently be examined for the underlying genetic factor(s) of the children, clinically normal children born to disease positive parents would not usually be studied for such factor(s), as exemplified in this study. Similarly, the frequent patient-to-patient transmission of the duplications/triplications would also be ascribed to ascertainment bias, because molecular studies would preferentially be performed in such families. Nevertheless, the apparently autosomal dominant inheritance pattern of limb malformations in several families may still suggest the relevance of a non-physiological *cis*-acting modifier(s) (see Models A and E in Figure 3). It is possible that such a modifier(s), once transferred onto the duplication/triplication positive chromosome 17, is usually co-transmitted with the duplications/triplications, leading to a specific condition in which the effects of *BHLHA9* overdosage frequently but not invariably exceed the threshold for the development of limb malformations in offsprings with the duplications/triplications.

Remarks

Several matters should be pointed out in the present study. First, in contrast to diverse duplication sizes in non-Japanese populations [5-9], the size of the genomic segment subjected to duplications/triplications was identical in this study. Since families 1–27 were derived from various places of Japan, there is no selection bias in terms of a geographic distribution. Rather, since the small duplications/triplications identified in this study were not associated with developmental retardation, it is likely that they spread throughout Japan primarily via carriers with normal fitness and were found via patients with limb malformations. Obviously, this notion does not exclude the possible presence of other types of duplications/triplications at 17p13.3 in Japan. Second, except for the duplications/triplications at 17p13.3, we could reveal a homozygous *WNT10B* mutation (SHFM6) only in a single SHFM family and chromosome 10q24 duplications (SHFM3) only in three SHFM families. Thus, underlying factors are still unknown in the remaining 20 families, although tiny deletions and/or duplications affecting the known SHFM loci might have been overlooked because of the low resolution of the array. In addition, although all the probands had a normal karyotype, there might be cryptic translocations and/or inversions involving the known SHFM loci. Third, no deletion of *BHLHA9* was identified in the 51 probands and in the 200 control subjects. This argues against the relevance of *BHLHA9* haploinsufficiency to limb malformations, and coincides with the Japanese founder duplication being produced by a replication-mediated mechanism rather than an interchromatid/interchromosomal (but not an intrachromatid) NAHR that can lead to both deletions and duplications as a mirror image [17]. Furthermore, it remains to be determined (i) whether gain-of-function mutations (and possibly loss-of-function mutations as well) of *BHLHA9* are identified in patients with limb malformations, (ii) whether duplications/triplications involving *BHLHA9* underlie limb malformations other than SHFM, SHFLD, and GWC, and (iii) whether *BHLHA9*-containing duplications/triplications are also the most frequent underlying factors for limb malformations in non-Japanese populations.

Conclusions

The results imply that (i) duplications/triplications involving *BHLHA9* at chromosome 17p13.3 constitute a strong susceptibility factor for the development of a range of limb malformations including SHFM, SHFLD, and GWC; (ii) the Japanese founder duplication was generated by a replication-based mechanism and spread with subsequent triplication and haplotype modification through recombination-based mechanisms; and (iii) clinical variability appears to be due to multiple factors including the size of duplications/triplications. Thus, the present study provides useful information on the development of limb malformations.

Additional files

Additional file 1: Table S1. Primers utilized in this study.

Additional file 2: Figure S1. Real-time PCR analysis.

Additional file 3: Figure S2. *D17S1174* analysis in 200 Japanese control subjects, showing discontinuous distribution of the CA repeat numbers, as observed in the Japanese families with limb malformations.

Additional file 4: Table S2. *In silico* analysis for specific structures around the breakpoint-flanking regions and control regions.

Additional file 5: Table S3. Phenotypes in patients/subjects with increased copy number of *BHLHA9*.

Additional file 6: Figure S3. Genomic region encompassing *BHLHA9* examined in this study.

Additional file 7: Table S4. Polymorphism analysis of rs3951819 (A/G SNP) in *BHLHA9*.

Additional file 8: Table S5. Polymorphism analysis of rs34201045 (4 bp insertion) in *TP63*.

Additional file 9: Figure S4. Genomic basis of the Japanese founder copy number gain.

Abbreviations

AER: Apical ectodermal ridge; CEP17: Centromere of chromosome 17; CGH: Comparative genomic hybridization; Dup: Duplication; FoSTeS: Fork stalling and template switching; GWC: Golfop-Wolfgang complex; L: Lower; LBD: Long bone defect; MMBIR: Microhomology-mediated break-induced replication; NAHR: Non-allelic homologous recombination; N.E.: Not examined; NHEJ: Non-homologous end-joining; qPCR: Quantitative real-time PCR; SF: Split foo17)t; SH: Split hand; SHFLD: SHFM with long bone deficiency; SHFM: Split-hand/foot malformation; Trip: Triplication; U: Upper.

Competing interests

The authors have nothing to declare.

Authors' contributions

Molecular analysis using human samples was performed by EN, HK, FK, RY, SN, SW, KY, TT, SS, MF, and TT, ST, and SY; clinical assessment and blood sampling by RK, HT, SM, TK, TH, MK, AS, KS, HO, NH, HN, EH, TN, HY, GN, and TO; design of this study and interpretations of the data by HA, SI, and TO; and paper writing by TO. All authors read and approved the final manuscript.

Acknowledgements

This work was supported in part by Grants-in-Aid for Scientific Research on Innovative Areas [22132004-A01] from the Ministry of Education, Culture, Sports, Science and Technology, by Grant for Research on Intractable Diseases from the Ministry of Health, Labor and Welfare [H24-048], and by Grants from National Center for Child Health and Development [23A-1, 24-7]. The funders had no role in study design, data collection and analysis, decision to publish, or preparation of the manuscript.

Author details

[1]Department of Pediatrics, Hamamatsu University School of Medicine, Hamamatsu 431-3192, Japan. [2]Laboratory of Bone and Joint Diseases, Center for Integrative Medical Sciences, RIKEN, Tokyo, Japan. [3]Department of Orthopedic Surgery, Tokyo, Japan. [4]Division of Medical Genetics, National Center for Child Health and Development, Tokyo, Japan. [5]Section of Clinical Genetics, Department of Pediatrics, Tenshi Hospital, Sapporo, Japan. [6]Department of Pediatrics, Central Hospital, Aichi Human Service Center, Kasugai, Japan. [7]Department of Human Genetics, Nagasaki University Graduate School of Biomedical Sciences, Nagasaki, Japan. [8]Department of Medical Genetics, Shinshu University School of Medicine, Matsumoto, Japan. [9]Department of Pediatrics, Keio University School of Medicine, Tokyo, Japan. [10]Department of Orthopedics, National Rehabilitation Center for Disabled Children, Tokyo, Japan. [11]Division of Medical Genetics, Saitama Children's Medical Center, Saitama, Japan. [12]Department of Rehabilitation Medicine, University of Tokyo, Tokyo, Japan. [13]Department of Genetic Counseling, Graduate School of Humanities and Sciences, Ochanomizu University, Tokyo, Japan. [14]Department of Orthopedic Surgery, Japanese Red Cross Nagoya Daiichi Hospital, Nagoya, Japan. [15]Department of Pediatrics, Dokkyo Medical University Koshigaya Hospital, Koshigaya, Japan. [16]Division of Medical Genetics, Tokyo, Japan. [17]Department of Pediatric Imaging, Tokyo Metropolitan Children's Medical Center, Tokyo, Japan. [18]Division of Neurology/Molecular Brain Science, Kobe University Graduate School of Medicine, Kobe, Japan. [19]Department of Systems Biomedicine, National Research Institute for Child Health and Development, Tokyo, Japan. [20]Department of Systems Biomedicine, Graduate School of Medical and Dental Sciences, Tokyo Medical and Dental University, Tokyo, Japan. [21]Department of Molecular Endocrinology, National Research Institute for Child Health and Development, Tokyo, Japan. [22]Present address: Laboratory of Metabolism Center for Cancer Research, National Cancer Institute, Bethesda, MD, USA.

Received: 15 April 2014 Accepted: 22 July 2014
Published online: 21 October 2014

References

1. Duijf PH, van Bokhoven H, Brunner HG: **Pathogenesis of split-hand/split-foot malformation.** *Hum Mol Genet* 2003, 12:R51–60.
2. Gurrieri F, Everman DB: **Clinical, genetic, and molecular aspects of split-hand/foot malformation: an update.** *Am J Med Genet A* 2013, 161A:2860–2672.
3. Lango Allen H, Caswell R, Xie W, Xu X, Wragg C, Turnpenny PD, Turner CL, Weedon MN, Ellard S: **Next generation sequencing of chromosomal rearrangements in patients with split-hand/split-foot malformation provides evidence for DYNC1/1 exonic enhancers of DLX5/6 expression in humans.** *J Med Genet* 2014, 51:264–267.
4. Lezirovitz K, Maestrelli SR, Cotrim NH, Otto PA, Pearson PL, Mingroni-Netto RC: **A novel locus for split-hand/foot malformation associated with tibial hemimelia (SHFLD syndrome) maps to chromosome region 17p13.1-17p13.3.** *Hum Genet* 2008, 123:625–631.
5. Armour CM, Bulman DE, Jarinova O, Rogers RC, Clarkson KB, DuPont BR, Dwivedi A, Bartel FO, McDonell L, Schwartz CE, Boycott KM, Everman DB, Graham GE: **17p13.3 microduplications are associated with split-hand/foot malformation and long-bone deficiency (SHFLD).** *Eur J Hum Genet* 2011, 19:1144–1151.
6. Klopocki E, Lohan S, Doelken SC, Stricker S, Ockeloen CW, Soares Thiele de Aguiar R, Lezirovitz K, Mingroni Netto RC, Jamsheer A, Shah H, Kurth I, Habenicht R, Warman M, Devriendt K, Kordass U, Hempel M, Rajab A, Mäkitie O, Naveed M, Radhakrishna U, Antonarakis SE, Horn D, Mundlos S: **Duplications of BHLHA9 are associated with ectrodactyly and tibia hemimelia inherited in non-Mendelian fashion.** *J Med Genet* 2012, 49:119–125.
7. Petit F, Andrieux J, Demeer B, Collet LM, Copin H, Boudry-Labis E, Escande F, Manouvrier-Hanu S, Mathieu-Dramard M: **Split-hand/foot malformation with long-bone deficiency and BHLHA9 duplication: two cases and expansion of the phenotype to radial agenesis.** *Eur J Med Genet* 2013, 56:88–92.
8. Curry CJ, Rosenfeld JA, Grant E, Gripp KW, Anderson C, Aylsworth AS, Saad TB, Chizhikov VV, Dybose G, Fagerberg C, Falco M, Fels C, Fichera M, Graakjaer J, Greco D, Hair J, Hopkins E, Huggins M, Ladda R, Li C, Moeschler J, Nowaczyk MJ, Ozmore JR, Reitano S, Romano C, Roos L, Schnur RE, Sell S, Suwannarat P, Svaneby D, *et al*: **The duplication 17p13.3 phenotype: analysis of 21 families delineates developmental, behavioral and brain abnormalities, and rare variant phenotypes.** *Am J Med Genet A* 2013, 161A:1833–1852.
9. Luk HM, Wong VC, Lo IF, Chan KY, Lau ET, Kan AS, Tang MH, Tang WF, She WM, Chu YW, Sin WK, Chung BH: **A prenatal case of split-hand malformation associated with 17p13.3 triplication - a dilemma in genetic counseling.** *Eur J Med Genet* 2014, 57:81–84.
10. Petit F, Jourdain AS, Andrieux J, Baujat G, Baumann C, Beneteau C, David A, Faivre L, Gaillard D, Gilbert-Dussardier B, Jouk PS, Le Caignec C, Loget P, Pasquier L, Porchet N, Holder-Espinasse M, Manouvrier-Hanu S, Escande F: **Split hand/foot malformation with long-bone deficiency and BHLHA9 duplication: report of 13 new families.** *Clin Genet* 2014, 85:464–469.
11. Kano H, Kurosawa K, Horii E, Ikegawa S, Yoshikawa H, Kurahashi H, Toda T: **Genomic rearrangement at 10q24 in non-syndromic split-hand/split-foot malformation.** *Hum Genet* 2005, 118:477–483.
12. Matsuyama J, Mabuchi A, Zhang J, Iida A, Ikeda T, Kimizuka M, Ikegawa S: **A pair of sibs with tibial hemimelia born to phenotypically normal parents.** *J Hum Genet* 2003, 48:173–176.
13. Kagami M, Sekita Y, Nishimura G, Irie M, Kato F, Okada M, Yamamori S, Kishimoto H, Nakayama M, Tanaka Y, Matsuoka K, Takahashi T, Noguchi M, Tanaka Y, Masumoto K, Utsunomiya T, Kouzan H, Komatsu Y, Ohashi H, Kurosawa K, Kosaki K, Ferguson-Smith AC, Ishino F, Ogata T: **Deletions and epimutations affecting the human 14q32.2 imprinted region in individuals with paternal and maternal upd(14)-like phenotypes.** *Nat Genet* 2008, 40:237–242.
14. Iida A, Okamoto N, Miyake N, Nishimura G, Minami S, Sugimoto T, Nakashima M, Tsurusaki Y, Saitsu H, Shiina M, Ogata K, Watanabe S, Ohashi H, Matsumoto N, Ikegawa S: **Exome sequencing identifies a novel INPPL1 mutation in opsismodysplasia.** *J Hum Genet* 2013, 58:391–394.
15. Cer RZ, Donohue DE, Mudunuri US, Temiz NA, Loss MA, Starner NJ, Halusa GN, Volfovsky N, Yi M, Luke BT, Bacolla A, Collins JR, Stephens RM: **Non-B DB v2.0: a database of predicted non-B DNA-forming motifs and its associated tools.** *Nucl Acids Res* 2013, 41:D94–D100.
16. Kornreich R, Bishop DF, Desnick RJ: **α-Galactosidase A gene rearrangements causing Fabry disease: identification of short direct repeats at breakpoints in an Alu-rich gene.** *J Biol Chem* 1990, 265:9319–9326.
17. Gu W, Zhang F, Lupski JR: **(2008) Mechanisms for human genomic rearrangements.** *Pathogenetics* 2008, 1:4.
18. Vissers LE, Bhatt SS, Janssen IM, Xia Z, Lalani SR, Pfundt R, Derwinska K, de Vries BB, Gilissen C, Hoischen A, Nesteruk M, Wisniowiecka-Kowalnik B, Smyk

M, Brunner HG, Cheung SW, van Kessel AG, Veltman JA, Stankiewicz P: **Rare pathogenic microdeletions and tandem duplications are microhomology-mediated and stimulated by local genomic architecture.** *Hum Mol Genet* 2009, **18**:3579–3593.
19. Hastings PJ, Ira G, Lupski JR: **A microhomology-mediated break-induced replication model for the origin of human copy number variation.** *PLoS Genet* 2009, **5**:e1000327.
20. Colnaghi R, Carpenter G, Volker M, O'Driscoll M: **The consequences of structural genomic alterations in humans: genomic disorders, genomic instability and cancer.** *Semin Cell Dev Biol* 2011, **2011**(22):875–885.
21. Ugur SA, Tolun A: **Homozygous WNT10b mutation and complex inheritance in Split-Hand/Foot Malformation.** *Hum Mol Genet* 2008, **17**:2644–2653.
22. Oort PJ, Warden CH, Baumann TK, Knotts TA, Adams SH: **Characterization of Tusc5, an adipocyte gene co-expressed in peripheral neurons.** *Mol Cell Endocrinol* 2007, **276**:24–35.
23. Manning JT, Scutt D, Wilson J, Lewis-Jones DI: **The ratio of 2nd to 4th digit length: a predictor of sperm numbers and concentrations of testosterone, luteinizing hormone and oestrogen.** *Hum Reprod* 1998, **13**:3000–3004.
24. Manning JT, Trivers RL, Singh D, Thornhill R: **The mystery of female beauty.** *Nature* 1999, **399**:214–215.
25. Williams TJ, Pepitone ME, Christensen SE, Cooke BM, Huberman AD, Breedlove NJ, Breedlove TJ, Jordan CL, Breedlove SM: **Finger-length ratios and sexual orientation.** *Nature* 2000, **404**:455–456.
26. Heald AH, Ivison F, Anderson SG, Cruickshank K, Laing I, Gibson JM: **Significant ethnic variation in total and free testosterone concentration.** *Clin Endocrinol* 2003, **58**:262–266.
27. Manning JT, Stewart A, Bundred PE, Trivers RL: **Sex and ethnic differences in 2nd to 4th digit ratio of children.** *Early Hum Dev* 2004, **80**:161–168.
28. Wang G, Vasquez KM: **Non-B DNA structure-induced genetic instability.** *Mutat Res* 2006, **598**:103–119.
29. Zhao J, Bacolla A, Wang G, Vasquez KM: **Non-B DNA structure-induced genetic instability and evolution.** *Cell Mol Life Sci* 2010, **67**:43–62.
30. Benko S, Gordon CT, Mallet D, Sreenivasan R, Thauvin-Robinet C, Brendehaug A, Thomas S, Bruland O, David M, Nicolino M, Labalme A, Sanlaville D, Callier P, Malan V, Huet F, Molven A, Dijoud F, Munnich A, Faivre L, Amiel J, Harley V, Houge G, Morel Y, Lyonnet S: **Disruption of a long distance regulatory region upstream of SOX9 in isolated disorders of sex development.** *J Med Genet* 2011, **48**:825–830.
31. Fraser FC: **Trinucleotide repeats not the only cause of anticipation.** *Lancet* 1997, **350**:459–460.

doi:10.1186/s13023-014-0125-5
Cite this article as: Nagata *et al.*: Japanese founder duplications/triplications involving *BHLHA9* are associated with split-hand/foot malformation with or without long bone deficiency and Gollop-Wolfgang complex. *Orphanet Journal of Rare Diseases* 2014 **9**:125.

ANNALS of Clinical and Translational Neurology
Open Access
ANA American Neurological Association

BRIEF COMMUNICATION

ABCG2 variant has opposing effects on onset ages of Parkinson's disease and gout

Hirotaka Matsuo[1], Hiroyuki Tomiyama[2], Wataru Satake[3], Toshinori Chiba[1], Hiroyuki Onoue[4], Yusuke Kawamura[1], Akiyoshi Nakayama[1], Seiko Shimizu[1], Masayuki Sakiyama[1], Manabu Funayama[2], Kenya Nishioka[2], Toru Shimizu[5], Kenichi Kaida[4], Keiko Kamakura[4,6], Tatsushi Toda[3], Nobutaka Hattori[2] & Nariyoshi Shinomiya[1]

[1]Department of Integrative Physiology and Bio-Nano Medicine, National Defense Medical College, Tokorozawa, Japan
[2]Department of Neurology, Juntendo University School of Medicine, Tokyo, Japan
[3]Division of Neurology/Molecular Brain Science, Kobe University Graduate School of Medicine, Kobe, Japan
[4]Department of Internal Medicine, National Defense Medical College, Tokorozawa, Japan
[5]Midorigaoka Hospital, Osaka, Japan
[6]Department of Physical Therapy, School of Health Sciences, Tokyo University of Technology, Tokyo, Japan

Correspondence
Hirotaka Matsuo, Department of Integrative Physiology and Bio-Nano Medicine, National Defense Medical College, 3-2 Namiki, Tokorozawa, Saitama 359-8513, Japan. Tel: +81-4-2995-1482; Fax: +81-4-2996-5187; E-mail: hmatsuo@ndmc.ac.jp

Funding Information
Supported by grants from the Ministry of Education, Culture, Sports, Science, and Technology of Japan, the Ministry of Health, Labour and Welfare of Japan, the Ministry of Defense of Japan, the Japan Society for the Promotion of Science, the Kawano Masanori Memorial Foundation for Promotion of Pediatrics, and the Gout Research Foundation of Japan.

Received: 6 November 2014; Accepted: 30 November 2014

Annals of Clinical and Translational Neurology 2015; 2(3): 302–306

doi: 10.1002/acn3.167

Abstract

Uric acid (urate) has been suggested to play a protective role in Parkinson's disease onset through its antioxidant activity. Dysfunction of ABCG2, a high-capacity urate exporter, is a major cause for early-onset gout based on hyperuricemia. In this study, the effects of a dysfunctional *ABCG2* variant (Q141K, rs2231142) were analyzed on the ages at onset of gout patients ($N = 507$) and Parkinson's disease patients ($N = 1015$). The Q141K variant hastened the gout onset ($P = 0.0027$), but significantly associated with later Parkinson's disease onset ($P = 0.025$). Our findings will be helpful for development of more effective prevention of Parkinson's disease.

Introduction

Parkinson's disease (PD) is a multifactorial disease characterized by selective cell death of dopaminergic neurons. Oxidative stress is well known to be one of the major causes of PD development.[1] On the other hand, uric acid (UA), which has an antioxidant effect on the central nervous system (CNS), may play a protective role in onset and development of PD.[2,3] Gout, a consequence of hyperuricemia, is also associated with a lower risk of PD.[4] Previously, common dysfunctional variants of ATP-binding cassette transporter, sub-family G, member 2 (*ABCG2*, also known as *BCRP*), a urate transporter gene,[5,6] have been revealed to be a major cause of early-onset gout.[7] The common variant (Q141K, rs2231142) of *ABCG2* is proven to be a dysfunctional variant by in vitro functional studies.[5,6]

This study aimed to evaluate whether the Q141K variant of *ABCG2* could delay the age at onset (AAO) of PD in a relatively large population of Japanese patients.

Patients and Methods

Study participants

This study was approved by the institutional ethical committees, and all procedures involved in this study were performed in accordance with the Declaration of Helsinki. Informed consent in writing was obtained from each subject participating in this study. A total of 1015 PD patients (464 male and 548 female) and 507 gout male patients was collected and then genetically analyzed. PD patients were collected in Juntendo University (Tokyo, Japan) and Kobe University (Kobe, Japan). Diagnosis of PD was made by board-certified neurologists of the Japanese Society of Neurology, based on the presence of at least two cardinal features of PD with no secondary cause, no levodopa unresponsiveness, or no early signs of more extensive nervous system involvement.[8] Clinically defined gout cases were collected in the Kyoto Industrial Health Association (Kyoto, Japan).

Genetic analysis

Genomic DNA was extracted from whole peripheral blood cells.[9] For PD patients, genotyping of Q141K (rs2231142) in *ABCG2* gene was performed by direct sequencing using the following primers: forward, 5′-ATGGAGTTAACTGTCATTTGC-3′, and reverse, 5′-CACGTTCATATTATGTAACAAGCC-3′. DNA sequencing analysis was performed with a 3130xl Genetic Analyzer[10] (Life Technologies Corporation, Carlsbad, CA). The genotyping data of PD patients collected in Kobe University were obtained from the result of previous GWAS[11] using the Illumina Infinium HumanHap550 array (Illumina, Inc., San Diego, CA). For gout patients, genotyping of Q141K in *ABCG2* gene was performed by TaqMan assay (Life Technologies Corporation) with a LightCycler 480 (Roche Diagnostics, Mannheim, Germany).[12,13]

Statistical analysis

In the statistical analysis, SPSS v.17.0J (IBM Japan Inc., Tokyo, Japan) was used for all calculations. Regression analysis was used for the association analysis.

Results

The results of genotyping of gout and PD patients are shown in Table 1. Figure 1 shows the AAO of gout and PD participants of each genotype of *ABCG2* Q141K. The AAO (mean ± standard error) of gout were 40.4 ± 1.1 years old, 42.0 ± 0.7 years old, and 45.0 ± 1.1 years old for patients with Q141K homozygous (A/A), heterozygous (C/A) mutation, and without Q141K mutation (C/C), respectively. On the other hand, the AAO of PD were 58.5 ± 1.1 years old, 58.2 ± 0.5 years old, and 56.6 ± 0.5 years for patients with Q141K homozygous, heterozygous mutation, and without mutation, respectively. The AAO of gout with homozygous mutation was 4.6 years younger than those without Q141K mutation, while the AAO of PD with homozygous mutation was 1.6 years older than those without Q141K mutation.

The Q141K mutation of *ABCG2* hastened the onset of gout significantly ($P = 0.0027$; see Fig. 1A); on the contrary, this variant significantly delayed the PD onset ($P = 0.025$; see Fig. 1B).

Discussion

This study revealed for the first time that a common dysfunctional variant of *ABCG2* (Q141K, rs2231142) has surprisingly differential effects on two common diseases, significantly delaying the AAO of PD, while hastening that of gout. *ABCG2* encodes ATP-dependent transporter for urate excretion both in gut[14,15] and kidney.[16] Molecular functional studies revealed that ABCG2 dysfunction elevates serum UA levels.[5,6] As UA is the strong antioxidant, ABCG2 dysfunction might have a neuroprotective effect. In fact, our study showed that the dysfunctional variant of this UA-related gene, *ABCG2*, could have a protective effect against PD, which is wholly consistent with the previous studies suggesting that the higher levels of serum UA are negatively correlated with the risk of PD[17] and its rate of progression.[18]

So far, only a few genetic analyses have been performed about the association between PD onset and UA-related genes.[19,20] However, there is no report demonstrating that

Table 1. Genotype of *ABCG2* variant Q141K (rs2231142) for gout and PD patients.

	N (%)				
Q141K (rs2231142[1])	C/C	C/A	A/A	Total	MAF
Gout cases	131 (25.8)	257 (50.7)	119 (23.5)	507 (100.0)	0.49
PD cases	509 (50.1)	425 (41.9)	81 (8.0)	1015 (100.0)	0.29

PD, Parkinson's disease; MAF, minor allele frequency.

[1]For alleles of rs2231142 (C for cytosine; A for adenine), allele A is the minor allele.

a single variant of *ABCG2* could significantly affect the AAO of PD.

Together with the antioxidant effect of UA, our results strongly support the hypothesis that UA should reduce the risk of PD as an antioxidant, because oxidative stress is involved in the pathogenesis of PD. In addition to its expression in gut and kidney, ABCG2 highly expresses in the blood brain barrier (BBB).[21] Therefore, we propose a physiological model that ABCG2 exports urate from the brain side to the blood side at BBB (see Fig. 2). Since ABCG2 dysfunction decreases urate excretion via gut[14,15] and kidney,[16] which results in serum UA elevation,[5,6,14,16] it therefore has a pathogenic effect on earlier onset of gout. Elevated serum UA also should result in elevated UA levels in CNS. In addition, ABCG2 dysfunction could decrease urate excretion via BBB that enhances the

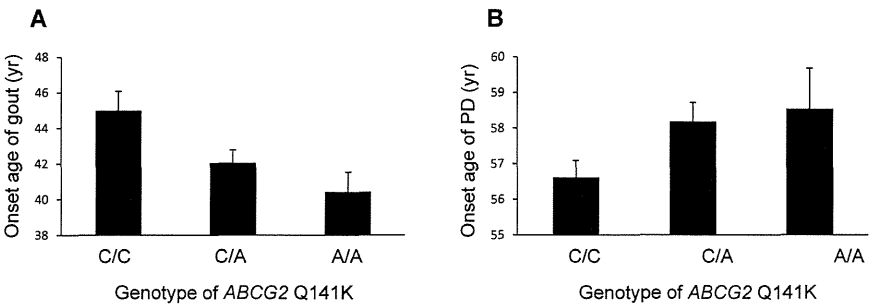

Figure 1. *ABCG2* dysfunctional variant (Q141K) and the age at onset (AAO) of gout/PD. The AAO of gout was significantly hastened as the number of minor alleles of Q141K increased ($P = 0.0027$); on the contrary, the AAO of PD was significantly delayed as the number of minor alleles of Q141K increased ($P = 0.025$). The AAO of gout with homozygous mutation (A/A) was 4.6 years younger than those without Q141K mutation (C/C). And the AAO of PD with homozygous mutation was 1.6 years older than those without Q141K mutation. Each bar represents the mean with standard error.

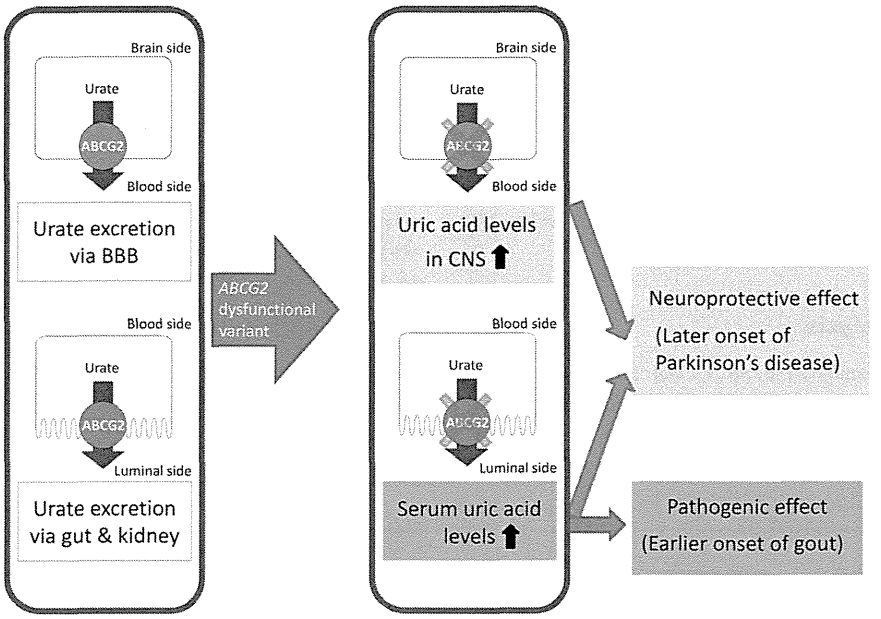

Figure 2. Contrary effects of ABCG2 dysfunction on PD and gout. ABCG2 is expressed in gut, kidney, and blood brain barrier (BBB) and exports urate. ABCG2 dysfunction in gut and kidney elevates the serum uric acid (UA) levels and subsequently causes gout. In this proposed model, ABCG2 dysfunction in BBB plays an important role on increasing UA levels in central nervous system (CNS), together with increased serum UA by ABCG2 dysfunction in gut and kidney.

elevation of UA levels in CNS as shown in our proposed model (see Fig. 2). In this model, ABCG2 dysfunction coordinately increases UA levels in CNS by the combined two differential mechanisms shown in Figure 2, although other UA-related gene variants have not been reported to have such differential mechanisms to elevate UA levels in CNS. Thus, the dysfunction of ABCG2 both in gut/kidney and BBB could cooperatively contribute to the elevated UA levels in CNS. These proposed differential mechanisms are consistent with our present result, which showed the differential effects on AAO of two common diseases, gout and PD. By these two differential mechanisms, therefore, ABCG2 dysfunction could have a significant neuroprotective effect for later onset of PD through increased UA, the strong antioxidant (see Fig. 2). That is why ABCG2 dysfunction could have significant effects on PD and be important in PD pathogenesis. Furthermore, the regulation of UA levels in serum and CNS could be applicable for prevention and therapy of PD.[22]

Acknowledgments

Supported by grants from the Ministry of Education, Culture, Sports, Science, and Technology of Japan, the Ministry of Health, Labour and Welfare of Japan, the Ministry of Defense of Japan, the Japan Society for the Promotion of Science, the Kawano Masanori Memorial Foundation for Promotion of Pediatrics, and the Gout Research Foundation of Japan. The authors thank all the participants involved in this study. We are also indebted to Y. Takada, T. Nakamura, H. Nakashima, Y. Sakurai, J. Abe, K. Gotanda, Y. Morimoto, H. Inoue, H. Ogata, S. Tatsukawa, Y. Shichijo, Y. Tanahashi, and A. Akashi, National Defense Medical College, Tokorozawa, Japan, for genetic analysis and enlightening discussion, and to T. Takada, the University of Tokyo Hospital, Tokyo, Japan, and Kimiyoshi Ichida, Tokyo University of Pharmacy and Life Sciences, Tokyo, Japan, for their helpful discussion.

Author Contribution

H. M., W. S., T. C., Y. K., A. N., S. S., M. S., T. T., and N. S. performed genetic analyses. H. T., W. S., H. O., M. F., K. N., T. S., K. Kaida., K. Kamakura., T. T., and N. H. performed clinical evaluations and medical record reviews. H. M. and T. C. wrote the paper. All authors contributed to data interpretation and manuscript preparation.

Conflicts of Interest

None declared.

References

1. Burkhardt CR, Weber HK. Parkinson's disease: a chronic, low-grade antioxidant deficiency? Med Hypotheses 1994;43:111–114.
2. Ascherio A, LeWitt PA, Xu K, et al. Urate as a predictor of the rate of clinical decline in Parkinson disease. Arch Neurol 2009;66:1460–1468.
3. Schlesinger I, Schlesinger N. Uric acid in Parkinson's disease. Mov Disord 2008;23:1653–1657.
4. Alonso A, Rodriguez LA, Logroscino G, Hernan MA. Gout and risk of Parkinson disease: a prospective study. Neurology 2007;69:1696–1700.
5. Woodward OM, Köttgen A, Coresh J, et al. Identification of a urate transporter, ABCG2, with a common functional polymorphism causing gout. Proc Natl Acad Sci USA 2009;106:10338–10342.
6. Matsuo H, Takada T, Ichida K, et al. Common defects of ABCG2, a high-capacity urate exporter, cause gout: a function-based genetic analysis in a Japanese population. Sci Transl Med 2009;1:5ra11.
7. Matsuo H, Ichida K, Takada T, et al. Common dysfunctional variants in ABCG2 are a major cause of early-onset gout. Sci Rep 2013;3:2014.
8. Bower JH, Maraganore DM, McDonnell SK, Rocca WA. Incidence and distribution of parkinsonism in Olmsted County, Minnesota, 1976–1990. Neurology 1999;52:1214–1220.
9. Matsuo H, Kamakura K, Saito M, et al. Familial paroxysmal dystonic choreoathetosis: clinical findings in a large Japanese family and genetic linkage to 2q. Arch Neurol 1999;56:721–726.
10. Chiba T, Matsuo H, Nagamori S, et al. Identification of a hypouricemia patient with SLC2A9 R380W, a pathogenic mutation for renal hypouricemia type 2. Nucleosides Nucleotides Nucleic Acids 2014;33:261–265.
11. Satake W, Nakabayashi Y, Mizuta I, et al. Genome-wide association study identifies common variants at four loci as genetic risk factors for Parkinson's disease. Nat Genet 2009;41:1303–1307.
12. Sakiyama M, Matsuo H, Shimizu S, et al. A common variant of leucine-rich repeat-containing 16A (LRRC16A) gene is associated with gout susceptibility. Hum Cell 2014;27:1–4.
13. Daimon M, Ji G, Saitoh T, et al. Large-scale search of SNPs for type 2 DM susceptibility genes in a Japanese population. Biochem Biophys Res Commun 2003;302:751–758.
14. Ichida K, Matsuo H, Takada T, et al. Decreased extra-renal urate excretion is a common cause of hyperuricemia. Nat Commun 2012;3:764.
15. Hosomi A, Nakanishi T, Fujita T, Tamai I. Extra-renal elimination of uric acid via intestinal efflux transporter BCRP/ABCG2. PLoS One 2012;7:e30456.

